


# Thermodynamically consistent model for diblock copolymer melts coupled with an electric field

Xiaowen Shen(沈晓文) and Qi Wang(王奇)

**Citation:**Chin. Phys. B, 2022, 31 (**4**): 048201. DOI: 10.1088/1674-1056/ac2728
Journal homepage: http://cpb.iphy.ac.cn; http://iopscience.iop.org/cpb

**What follows is a list of articles you may be interested in**

---

## Effect of grain boundary energy anisotropy on grain growth in ZK60 alloy using a 3D phase-field modeling

Yu-Hao Song(宋宇豪), Ming-Tao Wang(王明涛), Jia Ni(倪佳), Jian-Feng Jin(金剑锋), and Ya-Ping Zong(宗亚平)
Chin. Phys. B, 2020, 29 (**12**): 128201. DOI: 10.1088/1674-1056/abad1f

## Distribution of a polymer chain between two interconnected spherical cavities

Chao Wang(王超)†, Ying-Cai Chen(陈英才), Shuang Zhang(张爽), Hang-Kai Qi(齐航凯), and Meng-Bo Luo(罗孟波)‡
Chin. Phys. B, 2020, 29 (**10**): 108201. DOI: 10.1088/1674-1056/abaedc

## The n-type Si-based materials applied on the front surface of IBC-SHJ solar cells

Jianhui Bao(包建辉), Ke Tao(陶科), Yiren Lin(林苡任), Rui Jia(贾锐), Aimin Liu(刘爱民)
Chin. Phys. B, 2019, 28 (**9**): 098201. DOI: 10.1088/1674-1056/ab33ec

## Block copolymer morphologies confined by square-shaped particle: Hard and soft confinement

Qiyi Zhang(张启义), Wenyan Yang(杨文艳), Kaiyan Hu(胡凯燕)
Chin. Phys. B, 2016, 25 (**11**): 118201. DOI: 10.1088/1674-1056/25/11/118201

## Direct observation of $\lambda$ -DNA molecule reversal movement within microfluidic channels under electric field with single molecule imaging technique

Fengyun Yang(杨凤云), Kaige Wang(王凯歌), Dan Sun(孙聃), Wei Zhao(赵伟), Hai-qing Wang(王海青), Xin He(何鑫), Gui-ren Wang(王归仁), Jin-tao Bai(白晋涛)
Chin. Phys. B, 2016, 25 (**7**): 078201. DOI: 10.1088/1674-1056/25/7/078201

---

# Thermodynamically consistent model for diblock copolymer melts coupled with an electric field

Xiaowen Shen(沈晓文)[1,2] and Qi Wang(王奇)[3,†]

[1] *School of Physical and Mathematical Sciences, Nanjing Tech University, Nanjing* 211816, *China*
[2] *Beijing Computational Science Research Center, Beijing* 100193, *China*
[3] *Department of Mathematics, University of South Carolina, Columbia, SC* 29208, *USA*

(Received 26 May 2021; revised manuscript received 3 September 2021; accepted manuscript online 16 September 2021)

We present a thermodynamically consistent model for diblock copolymer melts coupled with an electric field derived using the Onsager linear response theory. We compare the model with the thermodynamically inconsistent one previously used for the coupled system to highlight their differences in describing transient dynamics.

**Keywords:** thermodynamical consistency, diblock copolymer melts, electric field, phase field model

**PACS:** 82.35.Jk, 82.60.Lf, 05.70.Ln, 64.70.qd **DOI:** 10.1088/1674-1056/ac2728

## 1. Introduction

The block copolymer comprises of two or more homopolymer subunits linked by covalent bonds. Copolymer melts consist of copolymers in liquid phase in high temperatures while copolymer solutions are mixtures of copolymers and solvents. In the diblock copolymer melt, the copolymer consists of polymer $A$ and polymer $B$ exclusively in two distinctive blocks. In the copolymer solution, either water or another homopolymer can serve as the additional phase, known as the solvent. Diblock copolymer systems can self-assemble into various ordered mesoscopic structures as the result of polymer-polymer and/or polymer-solvent interactions, which are often exploited in materials science and engineering, in particular, in nanotechnologies.[1–5]

The self-consistent field approach and associated numerical simulation have been proven to be effective means to investigate coarsening dynamics in copolymer systems. The seminal work of Ohta and Kawasaki[6] laid the foundation of phase field models for diblock copolymer systems. Ohta *et al.* also considered models for mixtures of diblock copolymers and a third immiscible phase.[7] Choksi and Ren[8,9] analyzed the models with rigorous mathematical techniques in minimization of free energy functionals. Coupling an external electric field or magnetic field to copolymer systems is one of the effective ways to manipulate and fabricate various nanostructured materials in materials' self-assembly involving copolymers and the nanoparticle phase.[10,11] Interesting mesoscopic morphologies can be obtained by quenching in melts or applying evaporation in solutions. The electric or magnetic field assisted self-assembly is a cutting-edge research in materials science and engineering today.

When the electric field is coupled to a diblock copolymer system, dipoles are induced so that the electric field is fully coupled to dynamics of the copolymer system. The existing phase field models for this system, however, have adopted an effective or simplified coupling term to include the electric field effect, resulting in models that do not have proper free energies not mention corresponding energy dissipation laws.[12–26] Because of this, we declare the resulting simplified models thermodynamically inconsistent. These thermodynamically inconsistent phase field models coupled with the electric field are based on two original papers,[27,28] where significant simplifications were carried out. The thermodynamical inconsistency may prevent one from accurately predicting transient morphology of the diblock copolymer system when coupled with the electric field. Note that thermodynamical consistency here refers to the positive entropy production principle or equivalently the free energy dissipation principle in isothermal cases in nonequilibrium thermodynamics expressed either as the generalized Onsager principle or as the second law of thermodynamics.[29–33] It is an important principle to follow when one devises quantitative models for any material systems and accompanying numerical algorithms for these models.

The rest of this paper is organized as follows. The mathematical model and accompanying second order numerical algorithms for diblock copolymer melts coupled with an electric field is developed in Section 2. In Section 3, the numerical investigations are carried out, where we compare relaxation dynamics of the thermodynamically consistent model developed with that of the existing thermodynamically inconsistent one. The conclusion is summarized in Section 4.

†Corresponding author. E-mail: qwang@math.sc.edu

© 2022 Chinese Physical Society and IOP Publishing Ltd 

## 2. Thermodynamically consistent model and numerical algorithms

### 2.1. Diblock copolymer melts coupled with an electric field

Consider the diblock copolymer melts in a fixed domain $\Omega \subset \mathbb{R}^d$ $(d = 2,3)$. We use $N_i$ to denote the polymerization degree of species $i = A$ and $B$. Denote the local volume fraction of polymer $A$ as $\phi_A = \phi$. We adopt the Ohta–Kawasaki free energy functional given in Ref. [6]

$$F[\phi] = \int_\Omega \left[\frac{\gamma}{2}|\nabla\phi|^2 + \chi\phi(1-\phi) + f(\phi)\right] \mathrm{d}\boldsymbol{x} + \frac{\alpha}{2}\int_\Omega\int_\Omega G(\boldsymbol{x},\boldsymbol{y})[\phi(\boldsymbol{x}) - \overline{\phi}][\phi(\boldsymbol{y}) - \overline{\phi}]\,\mathrm{d}\boldsymbol{y}\,\mathrm{d}\boldsymbol{x}, \quad (1)$$

where $f(\phi) = \frac{\phi}{N_A}\ln\phi + \frac{1-\phi}{N_B}\ln(1-\phi)$, $\overline{\phi} = \frac{1}{|\Omega|}\int_\Omega \phi\,\mathrm{d}\boldsymbol{x}$, and $G$ is the Green's function of the Laplacian operator with the homogeneous Neumann boundary condition, $\chi$ is the interaction parameter (a constant), $\alpha$ is the coupling constant parameter, and $\gamma$ measures the strength of the conformational entropy.

We define $\psi(\boldsymbol{x}) := -\int_\Omega G(\boldsymbol{x},\boldsymbol{y})[\phi(\boldsymbol{y}) - \overline{\phi}]\,\mathrm{d}\boldsymbol{y}$, satisfying Neumann boundary condition $\nabla\psi\cdot\boldsymbol{n}|_{\partial\Omega} = 0$, where $\boldsymbol{n}$ denotes the external unit normal of $\partial\Omega$. The time rate of change of the free energy is calculated as follows:

$$\frac{\mathrm{d}F}{\mathrm{d}t} = \int_\Omega [-\gamma\Delta\phi + \chi(1-2\phi) + f'(\phi) - \alpha\psi]\frac{\partial\phi}{\partial t}\,\mathrm{d}\boldsymbol{x} + \int_{\partial\Omega}\gamma\nabla\phi\cdot\boldsymbol{n}\frac{\partial\phi}{\partial t}\,\mathrm{d}s. \quad (2)$$

In the adiabatic case, the surface energy dissipation rate vanishes at Neumann boundary condition $\nabla\phi\cdot\boldsymbol{n}|_{\partial\Omega} = 0$. The chemical potential of the system is given by $\mu = n\delta F/\delta\phi = -\gamma\Delta\phi + \chi(1-2\phi) + f'(\phi) - \alpha\psi$.

Now we consider the additional free energy due to the existence of an electric field

$$F_\mathrm{e} = \int_\Omega \frac{1}{2}\boldsymbol{D}\cdot\boldsymbol{E}\,\mathrm{d}\boldsymbol{x} = \int_\Omega \frac{1}{2\varepsilon}\boldsymbol{D}\cdot\boldsymbol{D}\,\mathrm{d}\boldsymbol{x}, \quad (3)$$

where $\boldsymbol{D} = \varepsilon\boldsymbol{E}$ is the electric displacement, $\varepsilon$ is the dielectric constant of the material given by[27,28] $\varepsilon(\boldsymbol{x},t) = \varepsilon_0 + \varepsilon_1\varphi$, $\varphi = \phi_A - \phi_B - \overline{\phi}_A + \overline{\phi}_B = 2(\phi - \overline{\phi})$, $\varepsilon_0$ is the vacuum permittivity, and $\varepsilon_1$ is a material constant. Because of inhomogeneity of $\varepsilon(\boldsymbol{x},t)$, the electric field $\boldsymbol{E}$ inside the copolymer deviates from the applied electric field $\boldsymbol{E}_0$ and is given by $\boldsymbol{E} = \boldsymbol{E}_0 - \nabla\Phi$, where $\Phi$ is the electric potential for the induced electric field. $\Phi$ can be expressed in terms of $\varphi$ or $\phi$, by solving the following Poisson equation (Gauss theorem):

$$\begin{aligned}&\nabla\cdot\left[(\varepsilon_0 + \varepsilon_1\varphi)(\boldsymbol{E}_0 - \nabla\Phi)\right]\\ &= -\varepsilon_0\Delta\Phi + \varepsilon_1\boldsymbol{E}_0\cdot\nabla\varphi - \varepsilon_1\nabla\varphi\cdot\nabla\Phi - \varepsilon_1\varphi\Delta\Phi = 0, \end{aligned}\quad (4)$$

where $\Phi$ satisfies the Dirichlet boundary condition $\Phi|_{\partial\Omega} = 0$.

Referencing the work in Ref. [34], we have

$$\frac{\mathrm{d}F_\mathrm{e}}{\mathrm{d}t} = \int_\Omega -\frac{1}{2\varepsilon^2}|\boldsymbol{D}|^2\frac{\partial\varepsilon}{\partial\phi}\frac{\partial\phi}{\partial t}\,\mathrm{d}\boldsymbol{x} = \int_\Omega -\varepsilon_1|\boldsymbol{E}|^2\frac{\partial\phi}{\partial t}\,\mathrm{d}\boldsymbol{x}. \quad (5)$$

Since the total free energy is given by $F_\mathrm{total} = F + F_\mathrm{e}$, the time derivative of the total free energy becomes

$$\frac{\mathrm{d}F_\mathrm{total}}{\mathrm{d}t} = \int_\Omega (\mu + \mu_\mathrm{e})\frac{\partial\phi}{\partial t}\,\mathrm{d}\boldsymbol{x},$$

$$\mu_\mathrm{e} = \frac{\delta F_\mathrm{e}}{\delta\phi} = -\varepsilon_1|\boldsymbol{E}_0 - \nabla\Phi|^2, \quad (6)$$

under the adiabatic boundary conditions.

Using the Onsager principle, we obtain the electric field coupled diblock copolymer (E-BCP) melt model

$$\text{E-BCP model}: \begin{cases}\Delta\psi = \phi - \overline{\phi},\\ \nabla\cdot\left[(\varepsilon_0 + \varepsilon_1\varphi)(\boldsymbol{E}_0 - \nabla\Phi)\right] = 0,\\ \dfrac{\partial\phi}{\partial t} = M\Delta(\mu + \mu_\mathrm{e}),\end{cases} \quad (7)$$

where $M$ is the mobility coefficient. The adiabatic boundary conditions are given by $\boldsymbol{n}\cdot\nabla\phi|_{\partial\Omega} = 0$, $\nabla\psi\cdot\boldsymbol{n}|_{\partial\Omega} = 0$, $\Phi|_{\partial\Omega} = 0$, $\boldsymbol{n}\cdot\nabla(\mu + \mu_\mathrm{e})|_{\partial\Omega} = 0$. The free energy dissipation rate is given by

$$\frac{\mathrm{d}F_\mathrm{total}}{\mathrm{d}t} = -\int_\Omega M|\nabla(\mu + \mu_\mathrm{e})|^2\,\mathrm{d}\boldsymbol{x}. \quad (8)$$

This model is energy dissipative provided $M \geq 0$.

**Remark 1** If we drop nonlinear terms in Eq. (4) and approximate it by $\Delta\Phi = \frac{\varepsilon_1}{\varepsilon_0}\boldsymbol{E}_0\cdot\nabla\varphi$, we obtain a simplified electric field coupled diblock copolymer melt model

$$\begin{aligned}\frac{\partial\varphi}{\partial t} &= M\Delta\frac{\delta F}{\delta\phi} + M\frac{\varepsilon_1^2}{\varepsilon_0}(\boldsymbol{E}_0 - \nabla\Phi)\cdot\nabla\nabla\varphi\cdot\boldsymbol{E}_0\\ &\quad - M\varepsilon_1\nabla\nabla\Phi : \nabla\nabla\Phi^\mathrm{T}.\end{aligned} \quad (9)$$

If in addition, we drop the last term and use approximation $\boldsymbol{E}_0 - \nabla\Phi \approx \boldsymbol{E}_0$ in the above, we arrive at

$$\frac{\partial\varphi}{\partial t} = M\Delta\frac{\delta F}{\delta\phi} + M\frac{\varepsilon_1^2}{\varepsilon_0}\boldsymbol{E}_0\cdot\nabla\nabla\varphi\cdot\boldsymbol{E}_0. \quad (10)$$

When $\boldsymbol{E}_0 = [E_1, 0]^\mathrm{T} \in \mathbb{R}^2$, we recover the approximate model used in Ref. [12–26]

$$\frac{\partial\varphi}{\partial t} = M\Delta\frac{\delta F}{\delta\phi} + M\frac{\varepsilon_1^2}{\varepsilon_0}E_1^2\partial_x^2\varphi. \quad (11)$$

This is the simplified electric field coupled diblock copolymer (S-E-BCP) model. We summarize it as follows:

$$\text{S-E-BCP model}: \begin{cases}\Delta\psi = \phi - \overline{\phi},\\ \dfrac{\partial\phi}{\partial t} = M\Delta\mu + 4\dfrac{\varepsilon_1^2}{\varepsilon_0}ME_1^2\partial_x^2\phi.\end{cases} \quad (12)$$

We cannot find any proper free energy functional for this model that yields a negative energy dissipation rate. Hence, we regard this model as thermodynamically inconsistent!

### 2.2. Second order linear numerical algorithms

We present a 2n order energy dissipation rate preserving numerical algorithm to solve the thermodynamically consistent model numerically. We also use a numerical algorithm of the same order to solve the thermodynamically inconsistent model.

In order to mitigate potential numerical singularity, we regularize the logarithmic potential in the model by a $C^2$ piecewise function.[35] Specifically, for $0 < \sigma \ll 1$, we modified the bulk free energy as follows:

$$\hat{f}(\phi)=\begin{cases}\dfrac{1}{N_A}\Big(\dfrac{\phi^2}{2\sigma}+\phi\ln\sigma-\dfrac{\sigma}{2}\Big)+\dfrac{1-\phi}{N_B}\ln(1-\phi), & \phi\le\sigma,\\ \dfrac{\phi}{N_A}\ln\phi+\dfrac{1-\phi}{N_B}\ln(1-\phi), & \sigma\le\phi\le1-\sigma,\\ \dfrac{\phi}{N_A}\ln\phi+\dfrac{1}{N_B}\Big[\dfrac{(1-\phi)^2}{2\sigma}+(1-\phi)\ln\sigma-\dfrac{\sigma}{2}\Big], & \phi\ge1-\sigma.\end{cases}\tag{13}$$

To further confine $\phi\in(0,1)$, we add a hard wall potential $w(\phi)$ to the free energy such that $\widehat{F}=F+\int_\Omega w(\phi)\,\mathrm{d}\boldsymbol{x}$, where

$$w(\phi)=\begin{cases}0, & \phi\in(\varepsilon,1-\varepsilon),\\ 10^4(\phi-\varepsilon)^4(1-\varepsilon-\phi)^4, & \text{otherwise.}\end{cases}\tag{14}$$

We use $\sigma=\varepsilon=0.01$ in the following numerical simulation. However, for simplicity, we retain all original mathematical symbols in the presentation of algorithms.

### 2.2.1. Notations used in discretization

We consider a time domain $[0,T]$ for $T\in\mathbb{R}^+$. For $N_t\in\mathbb{Z}^+$, we define time step $\Delta t=T/N_t$ and the $n$-th step as $t_n=n\Delta t$ $(n=0,\ldots,N_t)$. Denote

$$\begin{aligned}&f^{n+\frac12}=(f^n+f^{n+1})/2,\\ &\delta_t^+f^n=(f^{n+1}-f^n)/\Delta t,\\ &\overline{f}^{n+\frac12}=(3f^n-f^{n-1})/2.\end{aligned}\tag{15}$$

For simplicity, we present a spatial discretization in 2D rectangular domain $\Omega=[0,L_x]\times[0,L_y]$. Let $N_x$ and $N_y$ be two positive integers. The domain $\Omega$ is uniformly partitioned with mesh sizes $h_x=L_x/N_x$ and $h_y=L_y/N_y$. The cell centered grid points are denoted by $\Omega_h=\{(x_i,y_j)|x_i=(i-1/2)h_x,y_j=(j-1/2)h_y,1\le i\le N_x,1\le j\le N_y\}$. We define the average and finite difference operators as follows:

$$\begin{aligned}&A_xf_{ij}=(f_{i-\frac12,j}+f_{i+\frac12,j})/2,\\ &A_yf_{ij}=(f_{i,j-\frac12}+f_{i,j+\frac12})/2,\\ &D_xf_{ij}=(f_{i+\frac12,j}-f_{i-\frac12,j})/h_x,\\ &D_yf_{ij}=(f_{i,j+\frac12}-f_{i,j-\frac12})/h_y,\\ &d_xf_{i-\frac12,j}=(f_{ij}-f_{i-1,j})/h_x,\\ &d_yf_{i,j-\frac12}=(f_{ij}-f_{i,j-1})/h_y,\\ &\Delta_hf_{ij}=(d_xD_x+d_yD_y)f_{ij}.\end{aligned}\tag{16}$$

The discrete inner product and norm are defined respectively by

$$(f,g)_h=\sum_{i=1}^{N_x}\sum_{j=1}^{N_y}f_{ij}g_{ij}h_xh_y,\quad \|f\|_h=\sqrt{(f,f)_h}.\tag{17}$$

The following summation-by-parts formulas are valid analogous to the integration-by-parts formulas in the continuous case:

$$(f,D_\alpha g)_h+(D_\alpha f,g)_h=0,$$

$$(f,d_\alpha g)_h+(d_\alpha f,g)_h=0,\quad \alpha=x,y,\tag{18}$$

when $f$ and $g$ satisfy proper boundary integrals with vanishing boundary conditions.

On the cell-centered grid, the boundary conditions we use in this study can be easily implemented by using the scheme and the discrete summation-by-parts formulae.

### 2.2.2. Linear implicit Crank–Nicolson schemes

We present a second order linear scheme based on the reformulated systems using the energy quadratization (EQ) method.[36] Firstly, we introduce an intermediate variable $q:=\sqrt{\frac{\phi}{N_A}\ln\phi+\frac{1-\phi}{N_B}\ln(1-\phi)+C}$, where $C\ge\frac{1}{N_A}+\frac{1}{N_B}>0$ is large enough to make $q>0$. Then, we have

$$\begin{aligned}F[\phi,q]=\int_\Omega\Big[&\frac{\gamma_1}{2}|\nabla\phi|^2+q^2-C+\chi\phi(1-\phi)\\ &-\frac{\alpha}{2}(\phi-\overline{\phi})\psi\Big]\,\mathrm{d}\boldsymbol{x}.\end{aligned}\tag{19}$$

For simplicity, we adopt the following notations in the description of the scheme:

$$\begin{aligned}&\mathcal{L}\phi=-\gamma_1\Delta\phi+\chi(1-2\phi)-\alpha\psi,\\ &(\overline{\mu}_{\mathrm{e}})_{ij}^{n+\frac12}=-\varepsilon_1\Big|\boldsymbol{E}_0-[d_xA_x,d_yA_y]^{\mathrm{T}}\overline{\boldsymbol{\Phi}}_{ij}^{n+\frac12}\Big|^2,\\ &F_h[\phi,\Phi,q]=\frac12(\phi,\mathcal{L}\phi)_h+(q,q)_h-C\\ &\qquad+\frac12\big(\varepsilon_0+\varepsilon_1(2\phi-2\overline{\phi}),|\boldsymbol{E}_0-\nabla\Phi|^2\big)_h.\end{aligned}\tag{20}$$

The EQ reformulated system of the E-BCP model (7) is given by

$$\begin{cases}\Delta\psi=\phi-\overline{\phi},\\ \nabla\cdot\big[(\varepsilon_0+\varepsilon_1\varphi)(\boldsymbol{E}_0-\nabla\Phi)\big]=0,\\ \dfrac{\partial\phi}{\partial t}=M\Delta\big[\mathcal{L}\phi+2qq'(\phi)+\mu_{\mathrm{e}}\big],\\ \dfrac{\partial q}{\partial t}=q'(\phi)\dfrac{\partial\phi}{\partial t}.\end{cases}\tag{21}$$

Applying the linear implicit Crank–Nicolson discretization in time, we obtain a second order EQ algorithm for the E-BCP model (7) as follows.

**Alorithm 1 E-BCP** Assuming $\phi^{n-1},\phi^n$ are known, we compute $\phi^{n+1}$ by

$$\begin{cases} \left(\dfrac{\varepsilon_0}{2\varepsilon_1}-\overline{\phi}+\overline{\phi}_{ij}^{n+\frac{1}{2}}\right)\Delta_h\overline{\Phi}_{ij}^{n+\frac{1}{2}}=\left(\boldsymbol{E}_0-[d_xA_x,d_yA_y]^{\mathrm{T}}\overline{\Phi}_{ij}^{n+\frac{1}{2}}\right)\cdot[d_xA_x,d_yA_y]^{\mathrm{T}}\overline{\phi}_{ij}^{n+\frac{1}{2}}, \\ \Delta_h\psi_{ij}^{n+\frac{1}{2}}=\phi_{ij}^{n+\frac{1}{2}}-\overline{\phi}, \\ \delta_t^+\phi_{ij}^n=M\Delta_h\left[\mathcal{L}_h\phi_{ij}^{n+\frac{1}{2}}+2q_{ij}^{n+\frac{1}{2}}q'(\overline{\phi}_{ij}^{n+\frac{1}{2}})+(\overline{\mu}_{\mathrm{e}})_{ij}^{n+\frac{1}{2}}\right], \\ \delta_t^+q_{ij}^n=q'(\overline{\phi}_{ij}^{n+\frac{1}{2}})\delta_t^+\phi_{ij}^n, \end{cases} \tag{22}$$

where $1\le i\le N_x$ and $1\le j\le N_y$.

This numerical scheme is thermodynamically consistent at the discrete level.

For completeness, we present a second order EQ algorithm for the S-E-BCP model (12) as follows.

**Algorithm 2 S-E-BCP** Assuming $\phi^{n-1},\phi^n$ are known, we compute $\phi^{n+1}$ through

$$\begin{cases} \Delta_h\psi_{ij}^{n+\frac{1}{2}}=\phi_{ij}^{n+\frac{1}{2}}-\overline{\phi}, \\ \delta_t^+\phi_{ij}^n=M\Delta_h\left[\mathcal{L}_h\phi_{ij}^{n+\frac{1}{2}}+2q_{ij}^{n+\frac{1}{2}}q'(\overline{\phi}_{ij}^{n+\frac{1}{2}})\right] \\ \qquad\qquad +4\dfrac{\varepsilon_1^2}{\varepsilon_0}ME_1^2d_xD_x\phi_{ij}^{n+\frac{1}{2}}, \\ \delta_t^+q_{ij}^n=q'(\overline{\phi}_{ij}^{n+\frac{1}{2}})\delta_t^+\phi_{ij}^n, \end{cases} \tag{23}$$

where $1\le i\le N_x$ and $1\le j\le N_y$.

This numerical scheme is not thermodynamically consistent at the discrete level.

## 3. Numerical results

We numerically compare differences of transient dynamics between E-BCP model (7) and S-E-BCP model (12). We fix $\Omega=[0,1]\times[0,1]$, $\Delta t=10^{-5}$, $h_x=h_y=1/128$ to conduct the numerical investigation. We set $N_A=3$, $N_B=7$, $\chi=6$, $\gamma=1.8\times10^{-3}$, $M=4\times10^{-3}$, $\varepsilon_0=1$, $\boldsymbol{E}_0=[10,0]^{\mathrm{T}}$ and $\varepsilon_1=0.2,\ 0.3$ respectively. The initial conditions are $\phi^0=\phi_A^0=0.3+10^{-3}\times\mathrm{rand}(x,y)$ and $\phi_B^0=1-\phi_A^0$, where $\mathrm{rand}(x,y)\in(-1,1)$ is a random number generator that follows the uniform distribution. Some phase portraits and induced electric fields at selected time slots are plotted in Figs. 1–4 and the total free energy of the E-BCP model is depicted in Fig. 5.

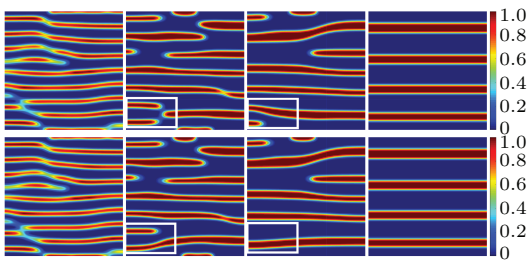


**Fig. 1.** Transient dynamics of phase separation and coarsening when $\varepsilon_1=0.2$ (S-E-BCP and E-BCP model in the 1st, 2nd row respectively). Color map of phase $\phi_A$ at $t=0.2,0.6,1,20$ respectively. The rectangles highlight the difference.

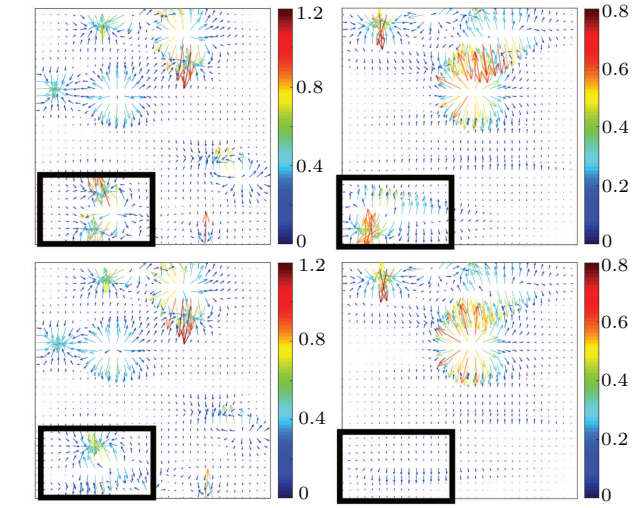


**Fig. 2.** Induced electric field $\nabla\Phi$ at $t=0.6,\ 1$ when $\varepsilon_1=0.2$ (S-E-BCP and E-BCP model in the 1st, 2nd row respectively). The rectangles highlight the difference.

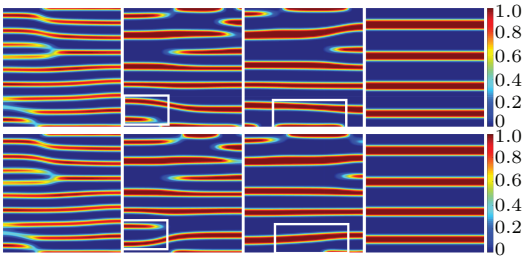


**Fig. 3.** Transient dynamics of phase separation and coarsening when $\varepsilon_1=0.3$ (S-E-BCP and E-BCP model in the 1st, 2nd row respectively). Color map of phase $\phi_A$ at $t=0.2,0.6,1,20$ respectively. The rectangles highlight the difference.

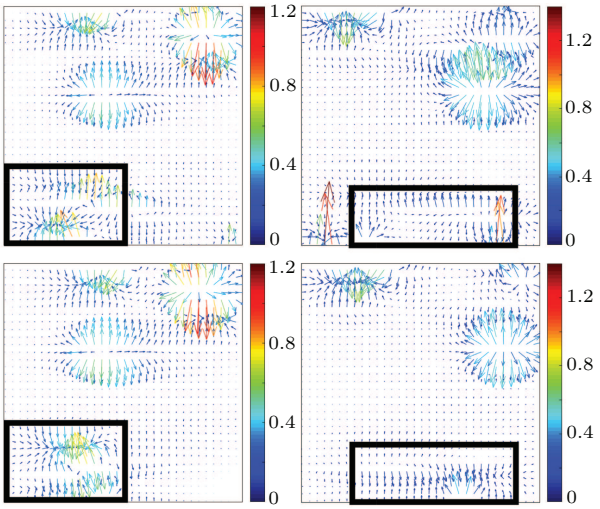


**Fig. 4.** Induced electric field $\nabla\Phi$ at $t=0.6,1$ when $\varepsilon_1=0.3$ (S-E-BCP and E-BCP model in the 1st, 2nd row respectively). The rectangles highlight the difference.

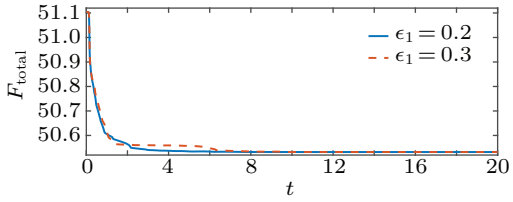



**Fig. 5.** Total free energy evolution in $t \in [0,20]$ of E-BCP model at 2 different values of $\varepsilon_1$.

When an electric field is coupled to copolymer melts, lamellae normally emerge in time. During transient from an irregular initial phase morphology to the lamellar pattern, branches or bridges are formed momentarily and annihilated eventually by the electric field. This is a process of defect removal in diblock copolymers assisted by external field in material processing, where one refers to the branches as defects. Under the influence of the electric field, structures coarsen to form stripes as well as defects in transient. Defects move along the direction of the electric field and disappear at the boundary of the domain driven by the electric field. The morphology of final structures forms a lamellar pattern with stripes along the direction of the electric field. For different parameter values $\varepsilon_1 = 0.2$ and 0.3, which parameterize material's dielectric responses to the electric field, we compute solutions of the two models with the same initial conditions up to when they reach steady states at $t = 20$. The two models generate somewhat different induced electric potentials at the same $\varepsilon_1$, leading to different transient structures in Figs. 1 and 3, respectively. For any $\varepsilon_1$, similar patterns emerge at the beginning $t = 0.2$ and similar steady states emerge at $t = 20$ between the two models, while transient dynamics are somewhat different (highlighted by rectangle marked areas). The total free energy curves of the thermodynamically consistent model (7) settle down to the steady state with time in Fig. 5.

## 4. Conclusion

In this paper, we derive a thermodynamically consistent phase field model for diblock copolymer melts coupled with the electric field, following fundamental principles of electrodynamics and the generalized Onsager principle. The resulting model respects an energy dissipation law for the total free energy. We then numerically compare the thermodynamically consistent model with an inconsistent one previously used to highlight their differences and thereby to emphasize the importance of thermodynamical consistency. The upshot of this study is that transient dynamics of thermodynamically consistent and inconsistent models can be quite different in morphological details, which can be significant in annealing for copolymer melts and therefore should not be ignored.

## Acknowledgements

Xiaowen Shen's research is partially supported by the National Natural Science Foundation of China (Grant Nos. 11971051 and U1930402). Qi Wang's research is partially supported by National Science Foundation grants (award DMS-1815921, 1954532 and OIA-1655740) and a GEAR award from SC EPSCoR/IDeA Program.

## References

[1] Parka C, Yoonb J and Thomas E L 2003 *Polymer* **44** 6725
[2] Liu M J, Li S B, Zhang L X and Wang X H 2010 *Chin. Phys. B* **19** 028101
[3] Zhang X M, Shen B F, Zhang L G and Shi Y 2021 *High Power Laser Science and Engineering* **9** e28
[4] Geng X B, Pan J X, Zhang J J, Sun M N and Cen J Y 2013 *Chin. Phys. B* **27** 058102
[5] Feng H B, Lu X Y, Wang W Y, Kang N G and Mays J W 2017 *Polymer* **9** 494
[6] Ohta T and Kawasaki K 1986 *Macromolecules* **19** 2621
[7] Ohta T and Nonomura M 1998 *Eur. Phys. J. B* **2** 57
[8] Choksi R and Ren X F 2003 *J. Stat. Phys.* **113** 151
[9] Choksi R and Ren X F 2005 *Physica D* **203** 100-119
[10] Pestera C W, Liedel C, Ruppel M and Böker A 2017 *Prog. Polym. Sci.* **64** 182
[11] Faghihi N, Mkhonta S, Elder K R and Grant M 2018 *Eur. Phys. J. B* **91** 55
[12] Kyrylyuk A V, Sevink G J A, Zvelindovsky A V and Fraaije J G E M 2003 *Macromol. Theory Simul.* **12** 508
[13] Lyakhova K S, Zvelindovsky A V and Sevink G J A 2004 *AIP Conf. Proc.* **708** 217
[14] Borja L J, Zurch M, Pemmaraju C D, Schultze M, Ramasesha K, Gandman A, Prell J S, Prendergast D, Neumark D M and Leone S R 2016 *United States*
[15] Lyakhova K S, Zvelindovsky A V and Sevink G J A 2006 *Macromolecules* **39** 3024
[16] Schmidt K, Schoberth H G, Schubert F, Hänsel H,Fischer F, Weiss T M, Sevink G J A, Zvelindovsky A V, Böker A and Krausch G 2007 *Soft Matter* **3** 448
[17] Ly D Q, Honda T, Kawakatsu T and Zvelindovsky A V 2007 *Macromolecules* **40** 2928
[18] Ly D Q, Honda T, Kawakatsu T and Zvelindovsky A V 2008 *Macromolecules* **41** 4501
[19] Wu X F and Dzenis Y A 2008 *Phys. Rev. E* **77** 031807
[20] Ding Y, Yang Q, Guo X, Wang S S, Gu F X, Fu J, Wan Q, Cheng J P and Tong L M 2009 *Opt. Express* **17** 21813
[21] Sevink G J A, Pinna M, Langner K M and Zvelindovsky A V 2011 *Soft Matter* **7** 5161
[22] Ly D Q, Pinna M, Honda T, Kawakatsu T and Zvelindovsky A V 2013 *J. Chem. Phys.* **138** 074904
[23] Orizaga S and Glasner K 2016 *Phys. Rev. E* **93** 052504
[24] Cheng Q, Yang X F and Shen J 2017 *J. Comput. Phys.* **341** 44
[25] Chen C J, Li X, Zhang J and Yang X F 2021 *Appl. Math. Comput.* **388** 125463
[26] Zhang J, Chen C J, Yang X F and Pan K J 2020 *J. Comput. Appl. Math.* **378** 112905
[27] Böker A, Elbs H, Hänsel H, Knoll A, Ludwigs S, Zettl H, Zvelindovsky A V, Sevink G J A, Urban V, Abetz V, Müller A H E and Krausch G 2003 *Macromolecules* **36** 8078
[28] Xu T, Zvelindovsky A V, Sevink G J A, Gang O, Ocko B, Zhu Y Q, Gido S P and Russell T P 2004 *Macromolecules* **37** 6980
[29] Onsager L 1931 *Phys. Rev.* **37** 405
[30] Onsager L 1931 *Phys. Rev.* **38** 2265
[31] Onsager L and Machlup S 1953 *Phys. Rev.* **91** 1505
[32] Yang X G, Li J, Forest M G and Wang Q 2016 *Entropy* **18** 202
[33] Wang Q 2021 *Frontiers and progress of current soft matter research* (Singapore: Springer Nature) pp. 101–132
[34] Landau L D and Lifshitz E M 1984 *Electrodynamics of continuous media*, 2nd edn. (Pergamon: Elsevier) pp. 34–85
[35] Yang X F and Zhao J 2019 *Comm. Comp. Phys.* **25** 703
[36] Zhao J, Yang X F, Gong Y Z, Zhao X P, Yang X G, Li J and Wang Q 2018 *Int. J. Numer. Anal. Mod.* **15** 884